



CARDIAC STRAINS FROM DENSE MRI:

EVALUATION OF SNR REQUIREMENTS AND STRAIN ERROR USING A COMPUTATIONAL PHANTOM

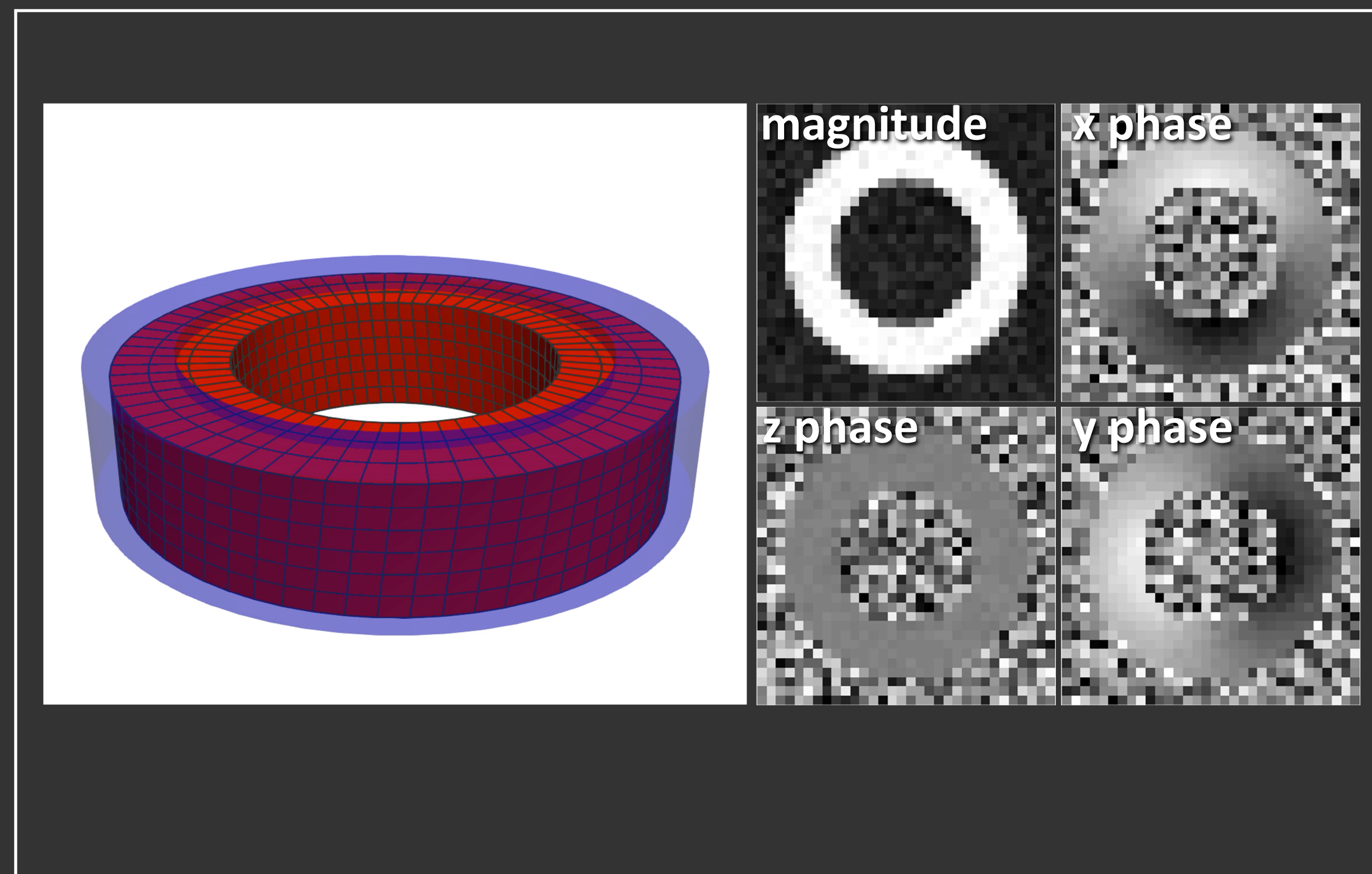
Ilya A. Verzhbinsky¹, Luigi E. Perotti², Kévin Moulin¹, Tyler E. Cork¹, Michael Loecher¹ and Daniel B. Ennis¹

¹Radiological Sciences Lab, Department of Radiology, Stanford University, Stanford, CA, USA

²Mechanical and Aerospace Engineering, University of Central Florida, Orlando, FL, USA



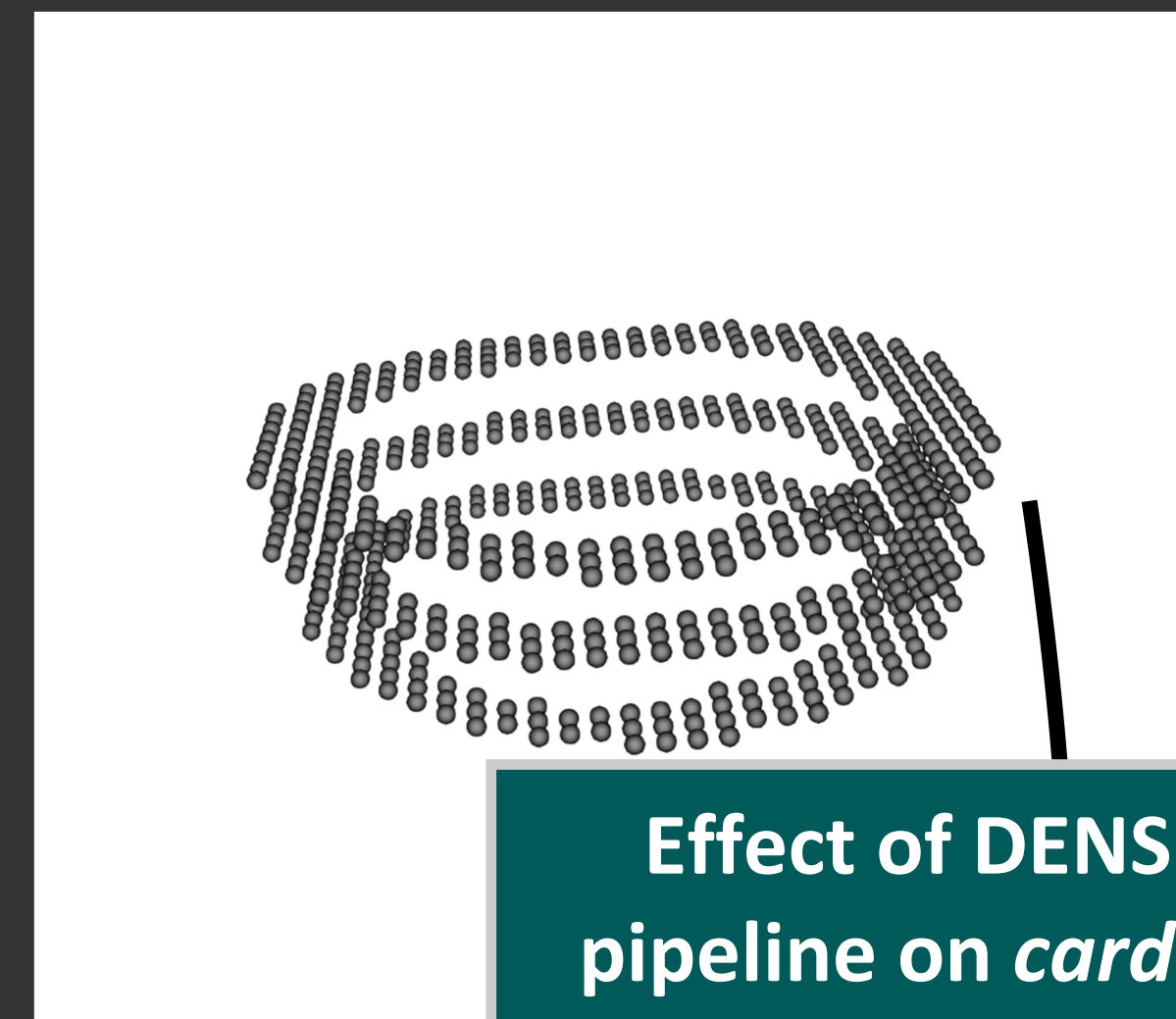
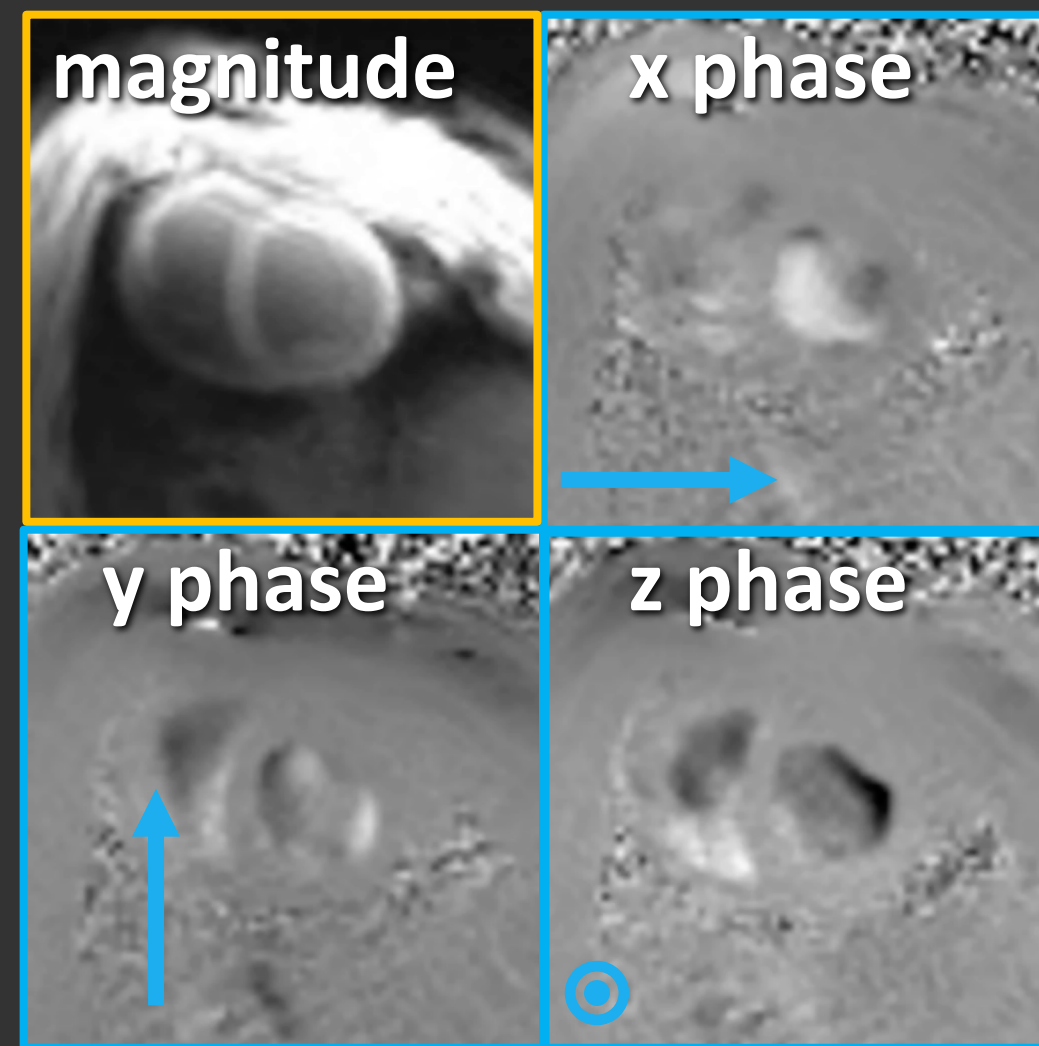
IMPACT: DENSE MRI encodes high-resolution cardiac tissue displacements into the phase of the complex MR signal. In this work, we present a computational deforming heart-like phantom to evaluate cardiac strains computed using a widely available, open-source DENSE Image Analysis Tool. These simulations can provide *a priori* estimates of required protocol parameters to achieve a target strain sensitivity in clinical studies.



INTRODUCTION

Introduction:

- DENSE MRI is effective for measuring regional cardiac strains in the clinic^{1,2} and in preclinical modeling studies evaluating myocardial stiffness³ and kinematics⁴.
- It remains unclear how image SNR specifically impacts measured cardiac strains along the circumferential (E_{cc}), radial (E_{rr}), longitudinal (E_{ll}) and cardiomyocyte aggregate (i.e. “fiber”) (E_{ff}) directions.

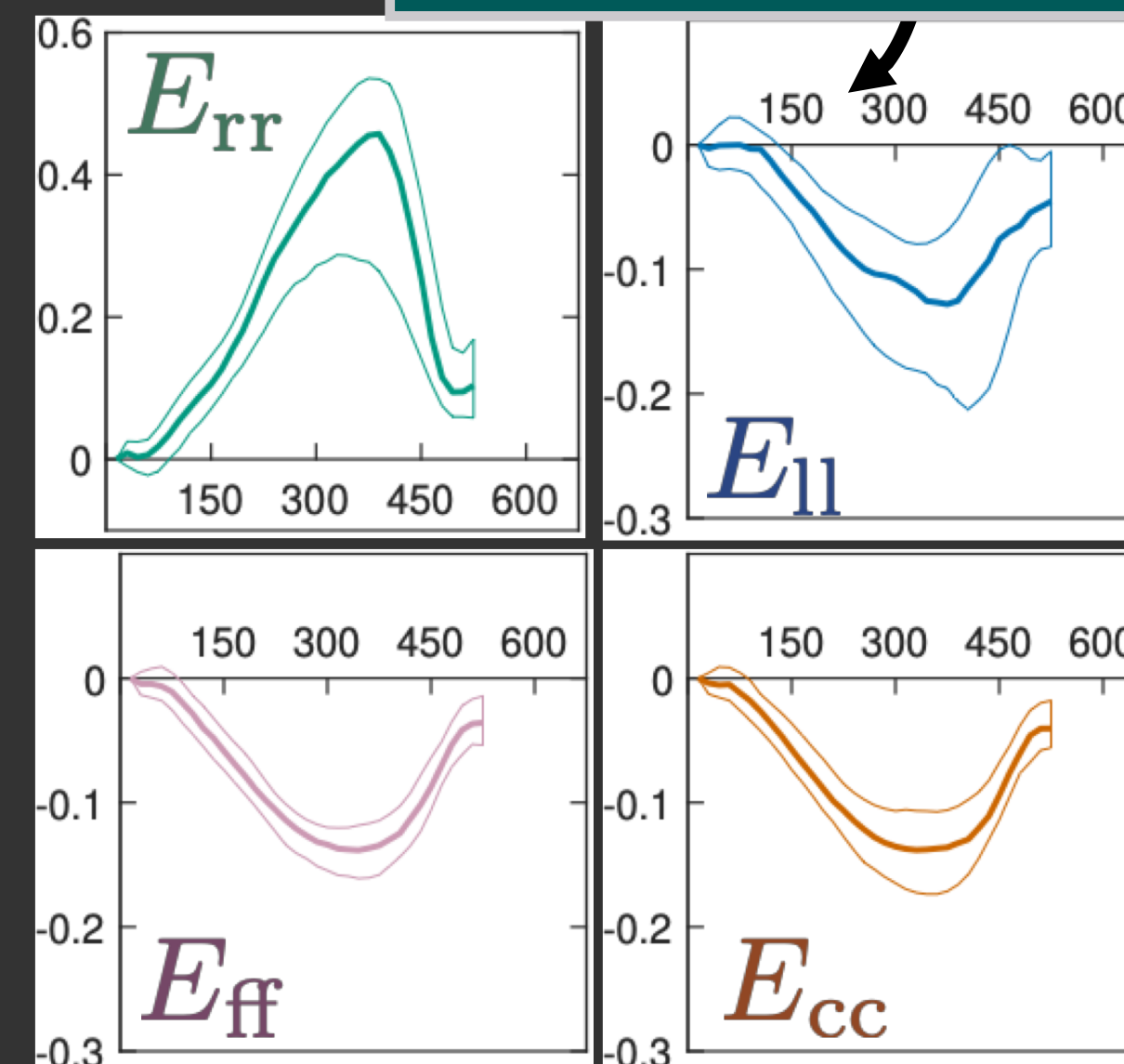


The objectives of this work were:

1. To quantify the accuracy and precision of cardiac strains computed using the most widely available, open-source DENSE Image Analysis Tool^{5,6}.
2. To quantify how image SNR propagates through the encoding and processing pipeline to impact the bias and range of computed E_{cc} , E_{rr} , E_{ll} and E_{ff} .

OBJECTIVES

- 1) Evaluate the accuracy and precision of DENSE processing pipeline.
- 2) Determine the sampling requirements for accurate strain measurements.



REFERENCES:

1. Aletras et al. Circ-Cardiovasc Imag 2011;74(4):425-34.
2. Bilchick et al. JACC 2014;63(16):1657-66.
3. Perotti et al. IJNMBE 2017;63(16):33(11):e2866.
4. Perotti et al. FIMH 2017;pp. 381-391.
5. Spottiswoode et al. IEEE TMI 2007;26(1):15-30.
6. Gilliam, A.D., Suever, J.D., and contributors (2016). DENSEanalysis. Retrieved from <https://github.com/denseanalysis/denseanalysis>

ACKNOWLEDGEMENTS:

Funding support from NIH K25 HL135408, NIH R01 HL131975 and NIH R01 HL131823.

For more information regarding an *in vivo* implementation of this work to compute aggregate cardiomyocyte strain, please see **Program #2104**.



Program #2103



METHODS

COMPUTATIONAL DEFORMING PHANTOM

Methods:

We use an axial-symmetric deforming heart-like computational phantom with time-resolved deformation defined by three analytical functions for radial, circumferential, and longitudinal motion.

$$\varphi_R = a_1 + R(1 + a_2) + a_3 * R^2;$$

$$\varphi_\theta = a_4(Z - Z_{bot}) / (Z_{top} - Z_{bot});$$

$$\varphi_Z = Z + a_5 Z$$

The parameters a_{1-5} were identified by minimizing the following objective function:

$$g = \sum_{i=1} w_1 (J_i - \bar{J})^2 + w_2 (E_{\ell\ell,i} - \bar{E}_{\ell\ell})^2 + w_3 (E_{cc,i} - \bar{E}_{cc})^2 + w_4 (E_{rr,i} - \bar{E}_{rr})^2 + w_5 (E_{ff,i} - \bar{E}_{ff})^2$$

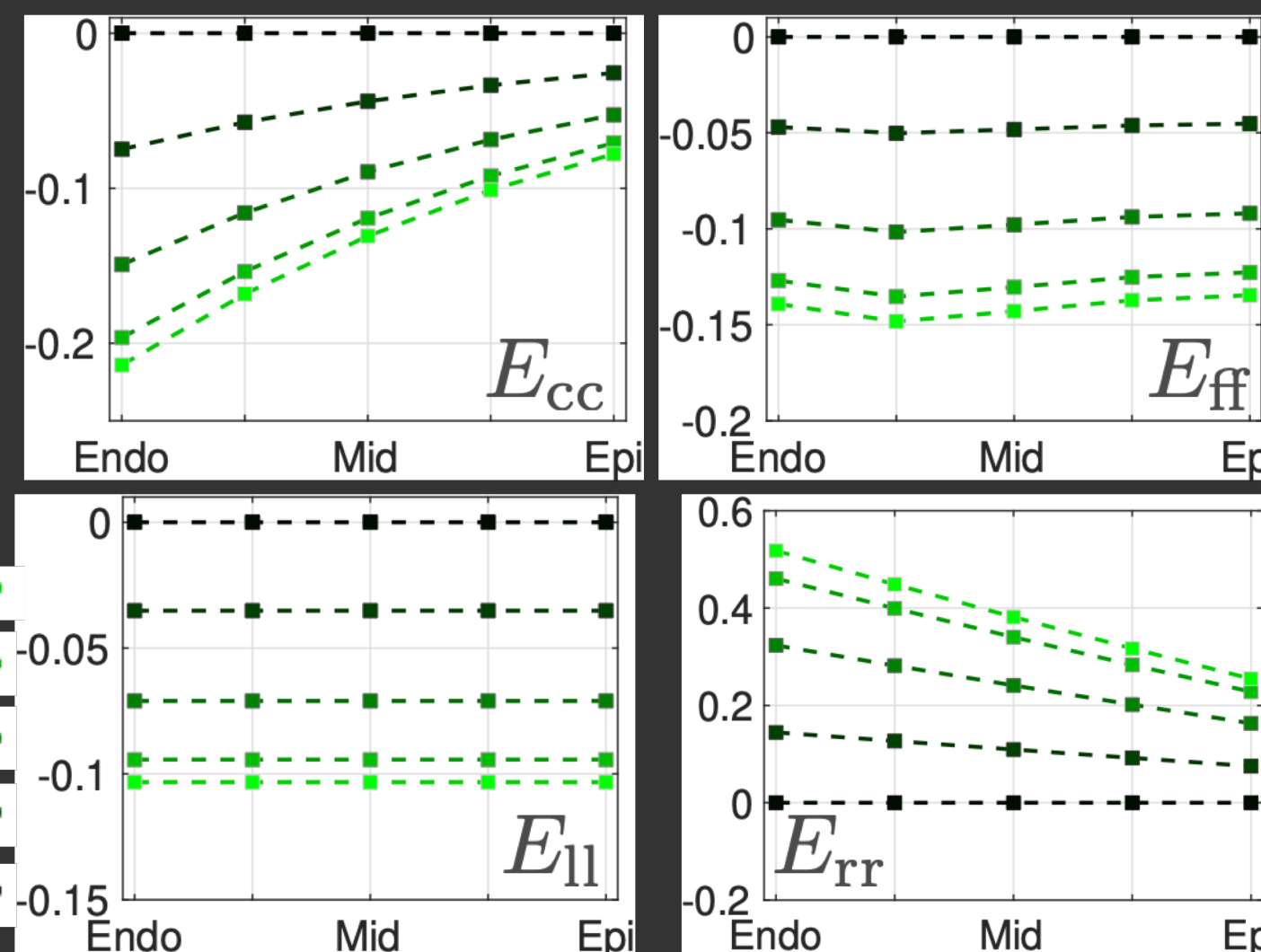
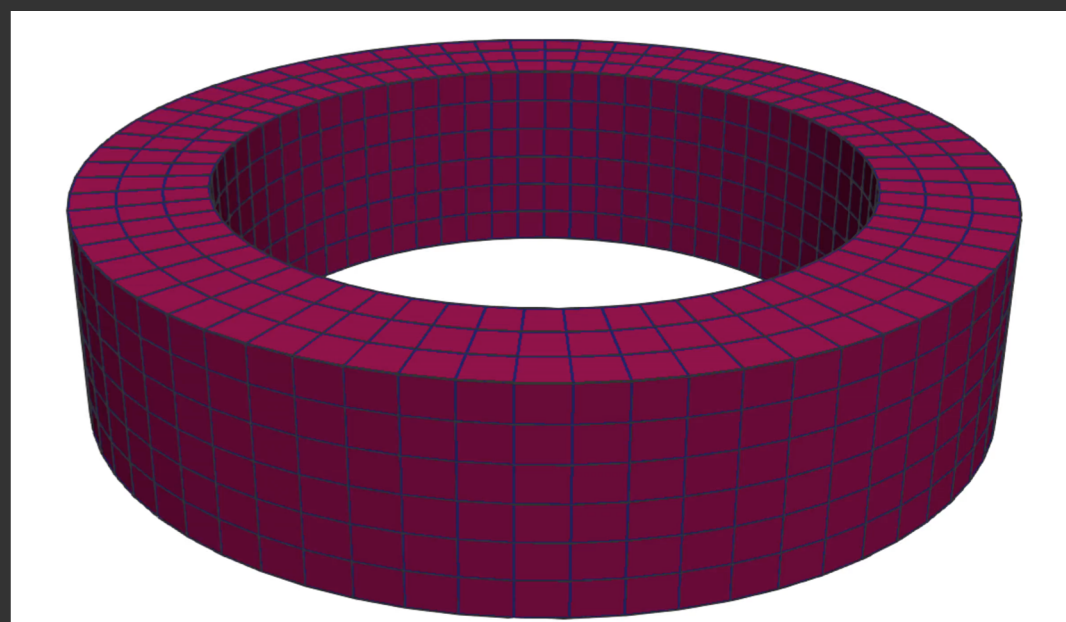
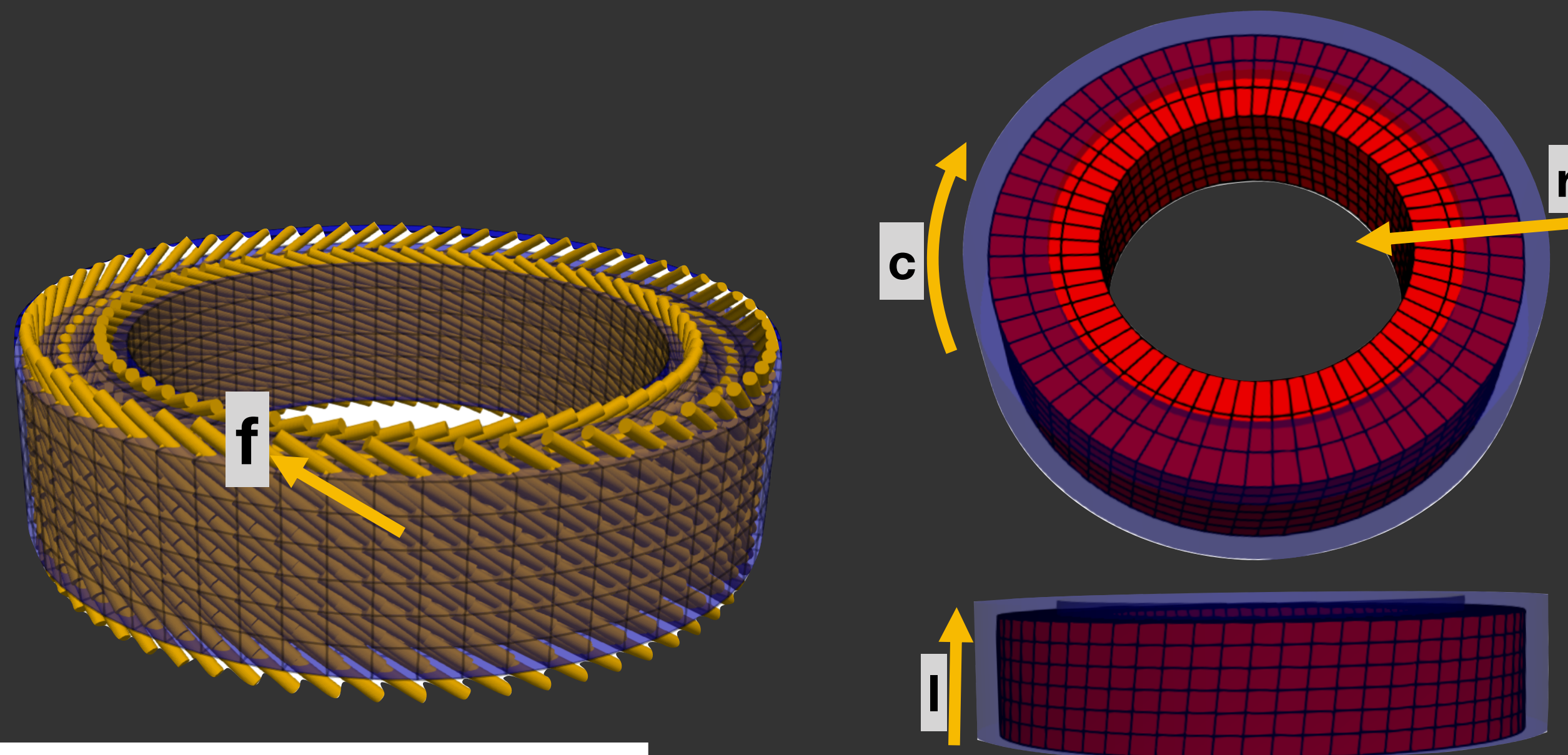
The target ground-truth peak systolic strains were calibrated based on strain reports from in vivo DENSE studies¹.

Phantom Parameters

	Epi	Mid	Endo
Fiber Angle (f)	-45	-9	37 [2]

$$R_{epi} = 35\text{mm} \quad Z_{top} = 16\text{mm}$$

$$R_{endo} = 25\text{mm} \quad Z_{bot} = 0\text{mm}$$



CARDIAC STRAINS FROM DENSE MRI

REFERENCES:

1. Zhong et al. MRM 2010;64(4):1089-97.
2. Ennis et al. J Biomech 2008;41(15):3219-24.

ACKNOWLEDGEMENTS:

Funding support from NIH K25 HL135408, NIH R01 HL131975 and NIH R01 HL131823.

For more information regarding an *in vivo* implementation of this work to compute aggregate cardiomyocyte strain, please see **Program #2104**.

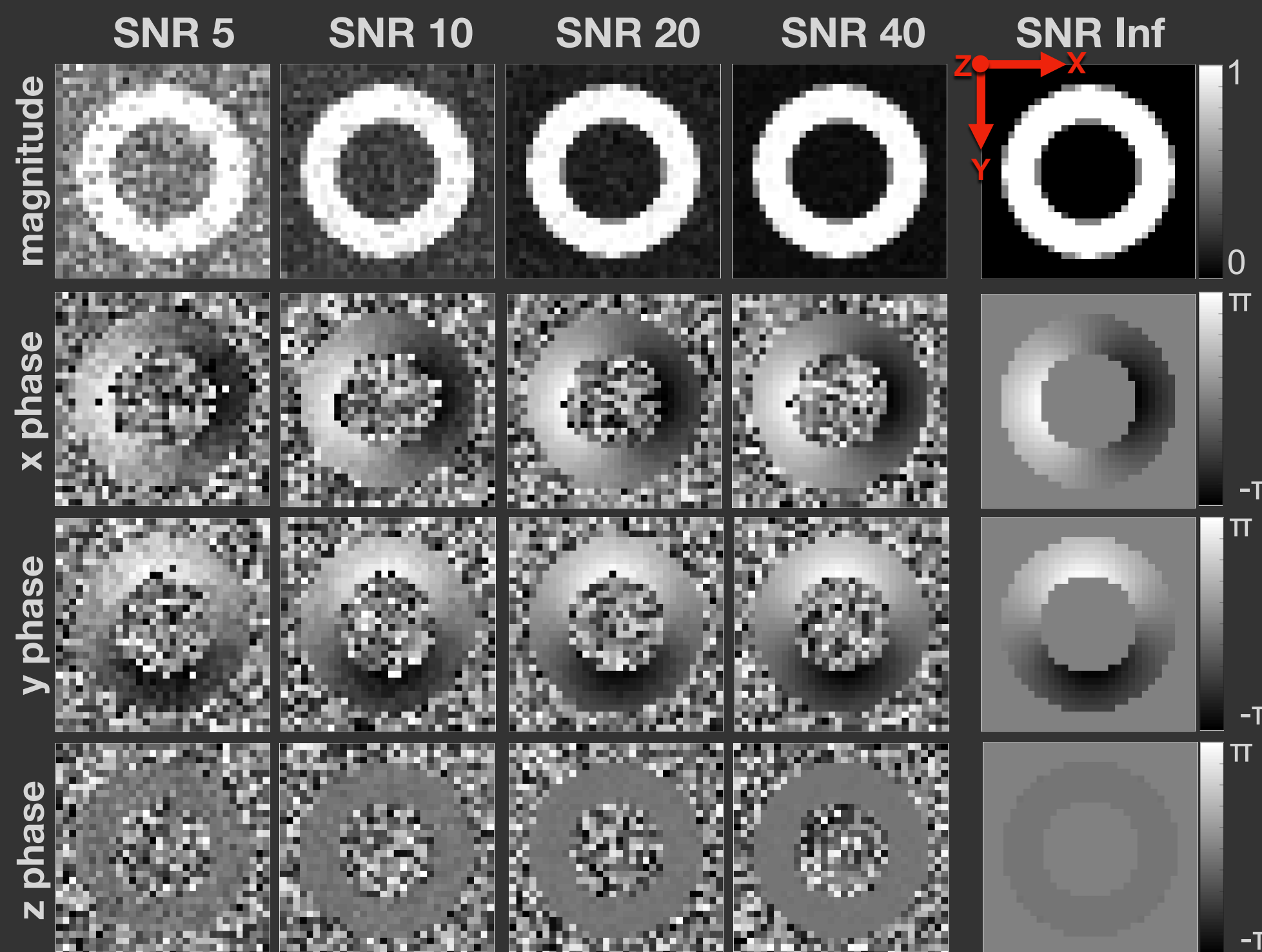


Program #2103

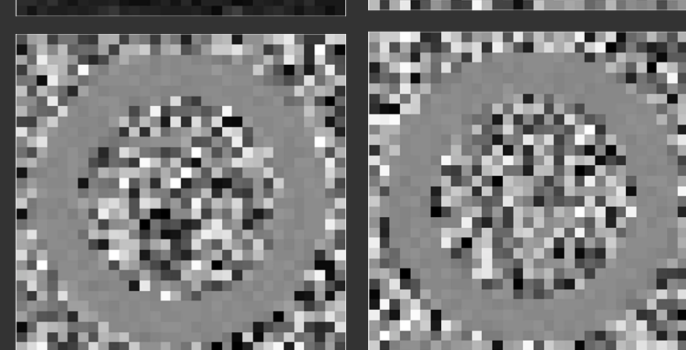
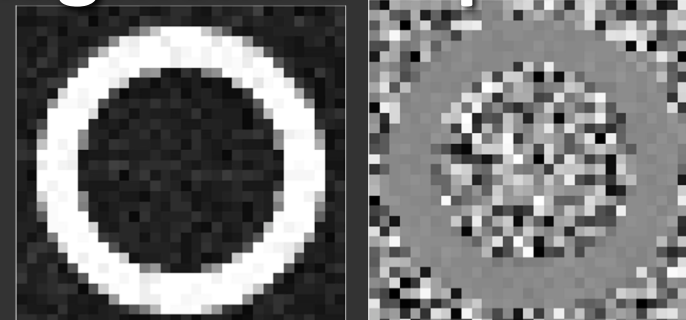


METHODS

DENSE IMAGE SIMULATION

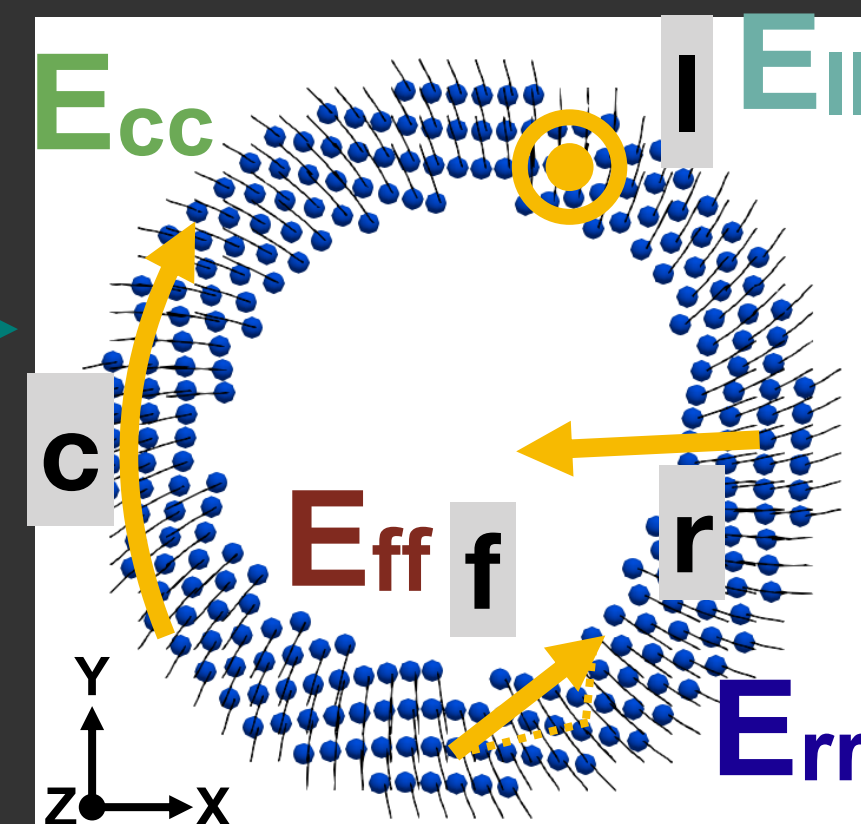


magnitude x phase



z phase y phase

DENSE Pipeline



CARDIAC STRAINS FROM DENSE MRI

Methods:

The phantom deformation field was subdivided into a grid of 2.5x2.5x8mm voxels at two slice locations, spaced 8mm from each other. The corresponding phase was computed by scaling the bulk displacement components according to an encoding strength of 0.08 cycles/mm. The signal magnitude was computed as the average magnitude across 12 intravoxel sampling points, assuming a signal of 0 for air and 1 for myocardium.

DENSE imaging typically employs a balanced 4-point encoding scheme. To properly account for noise, the phantom displacements were transformed into the corresponding balanced 4-point phase maps according to the encoding matrix outlined in Zhong et al.¹

$$\begin{bmatrix} \varphi_1 \\ \varphi_2 \\ \varphi_3 \\ \varphi_4 \end{bmatrix} = \begin{bmatrix} -\frac{\sqrt{3}}{3} & -\frac{\sqrt{3}}{3} & -\frac{\sqrt{3}}{3} & 1 \\ \frac{\sqrt{3}}{3} & \frac{\sqrt{3}}{3} & -\frac{\sqrt{3}}{3} & 1 \\ \frac{\sqrt{3}}{3} & -\frac{\sqrt{3}}{3} & \frac{\sqrt{3}}{3} & 1 \\ -\frac{\sqrt{3}}{3} & \frac{\sqrt{3}}{3} & \frac{\sqrt{3}}{3} & 1 \end{bmatrix} \begin{bmatrix} k_e D_x \\ k_e D_y \\ k_e D_x \\ \varphi_b \end{bmatrix}$$

Complex valued noise was added to the four phase maps for a range of five different SNRs (SNR = 5 - Inf). Finally, the resulting noise-injected complex images were encoded back into phase along x, y, and z. Each SNR simulation was repeated five times for strain analysis.

Green-Lagrange strain components were evaluated at 160 locations (X_q) between two simulated DENSE slices as:

$$E_{vv} = \frac{1}{2}(\vec{v} \cdot \mathbf{C}\vec{v} - 1),$$

where \mathbf{C} is the right Cauchy-Green deformation tensor, and v represents the direction along which the strain is computed, i.e., E_{cc} , E_{rr} , E_{ll} , E_{ff} . The strain bias, was computed at each X_q as:

$$\Delta E_{vv}(X_q) = E_{vv}^c(X_q) - E_{vv}^{an}(X_q),$$

REFERENCES:

- Zhong et al. MRM 2009;61(4):981-8.

ACKNOWLEDGEMENTS:

Funding support from NIH K25 HL135408, NIH R01 HL131975 and NIH R01 HL131823.

For more information regarding an *in vivo* implementation of this work to compute aggregate cardiomyocyte strain, please see **Program #2104**.

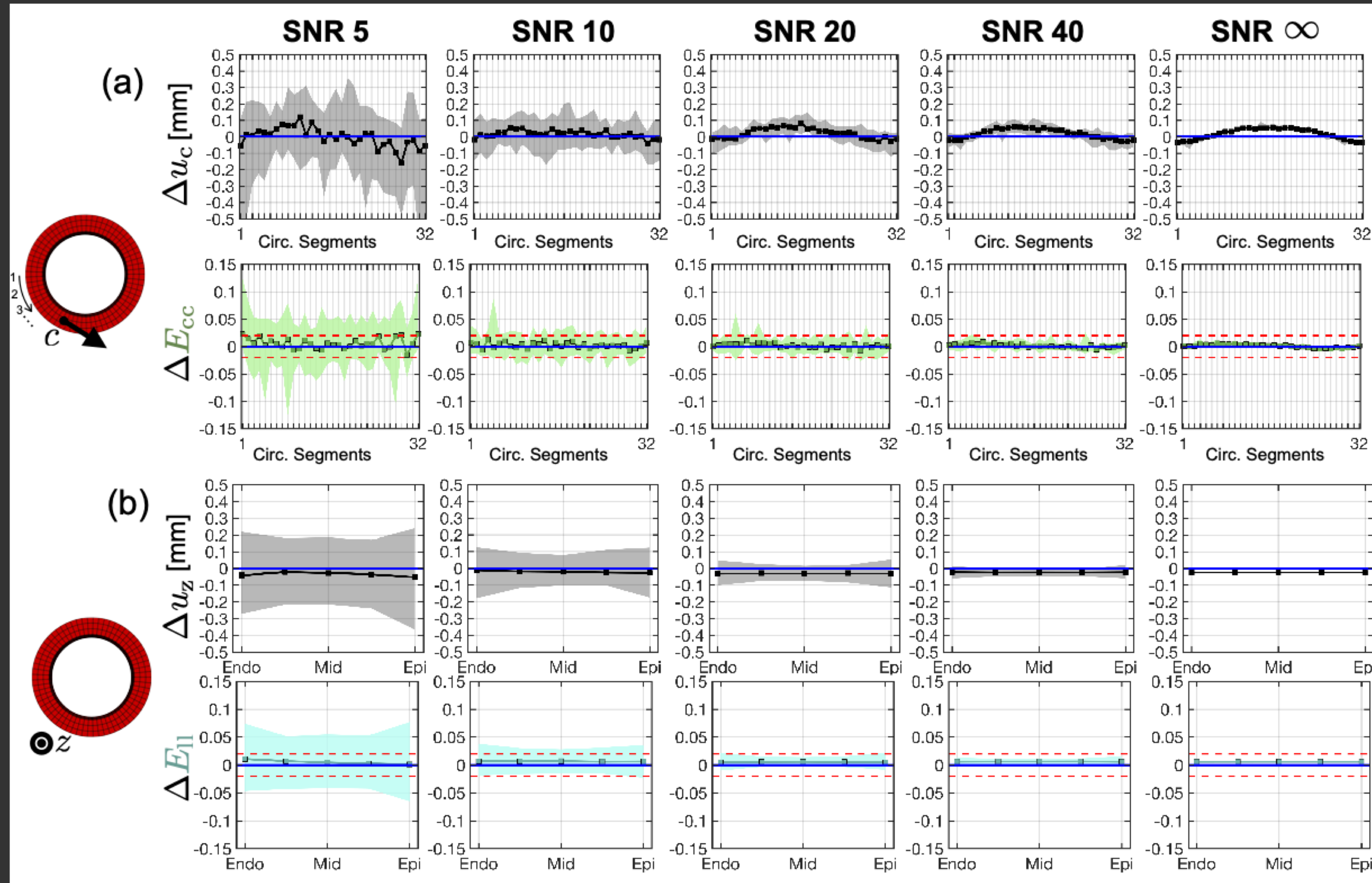


Program #2103



RESULTS

Figure 1 - Strain and displacement bias in the circumferential, and longitudinal directions across a range of SNRs. (a) Circumferential displacement (top) and strain (bottom) bias across 32 equal circumferential segments. The numbering of each segment is ordered in a counter-clockwise manner beginning at nine o'clock on the cylindrical phantom (left diagram). (b) Longitudinal displacement (top) and strain (bottom) bias from epicardium to endocardium. Squares are strain bias medians and shaded regions are the 95%-CI of strain bias (i.e., the tolerance). Blue and red horizontal lines represent, respectively, 0 median strain bias and +0.020 to -0.020 strain tolerance.



ACKNOWLEDGEMENTS:

Funding for this work was provided by NIH R01 HL131975 and HL131823 to DBE.

For more information regarding an *in vivo* implementation of this work to compute aggregate cardiomyocyte strain, please see **Program #2104**.

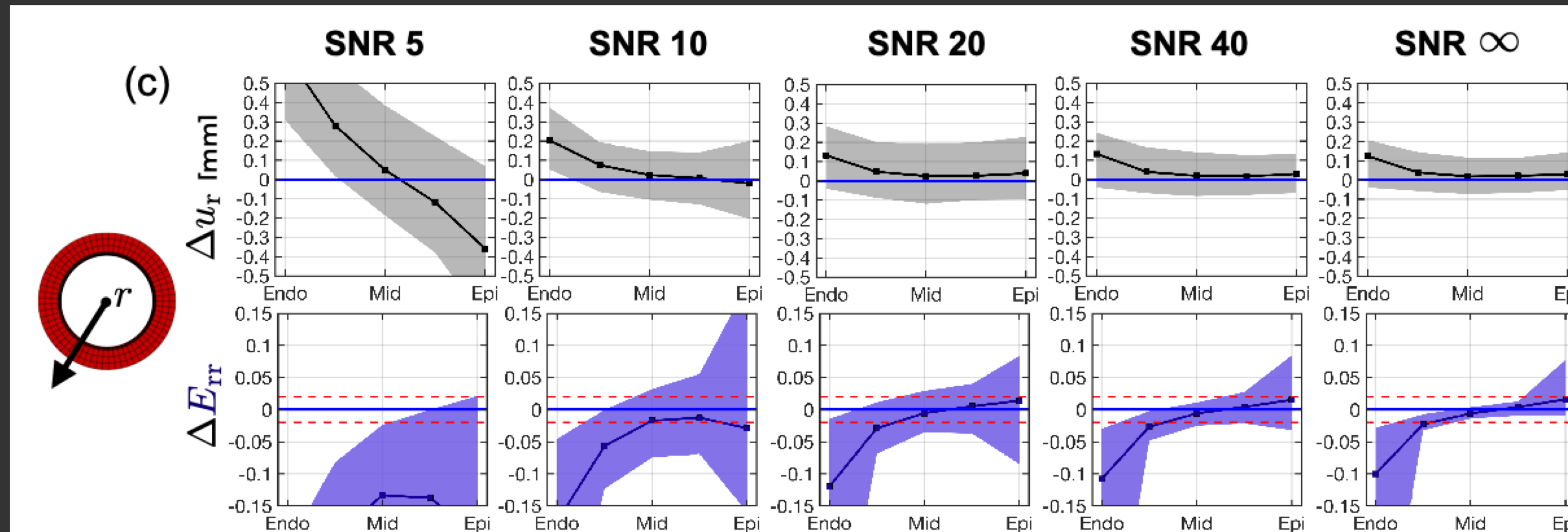


Program #2103



RESULTS

Figure 2 - Strain and displacement bias in the radial direction across a range of SNRs. (c) Radial displacement (top) and strain (bottom) bias from epicardium to endocardium. Squares are strain bias medians and shaded regions are the 95%-CI of strain bias (i.e., the tolerance). Blue and red horizontal lines represent, respectively, 0 median strain bias and +0.020 to -0.020 strain tolerance.



ACKNOWLEDGEMENTS:
Funding for this work was provided by NIH R01 HL131975 and HL131823 to DBE.

For more information regarding an *in vivo* implementation of this work to compute aggregate cardiomyocyte strain, please see **Program #2104**.



Program #2103



RESULTS

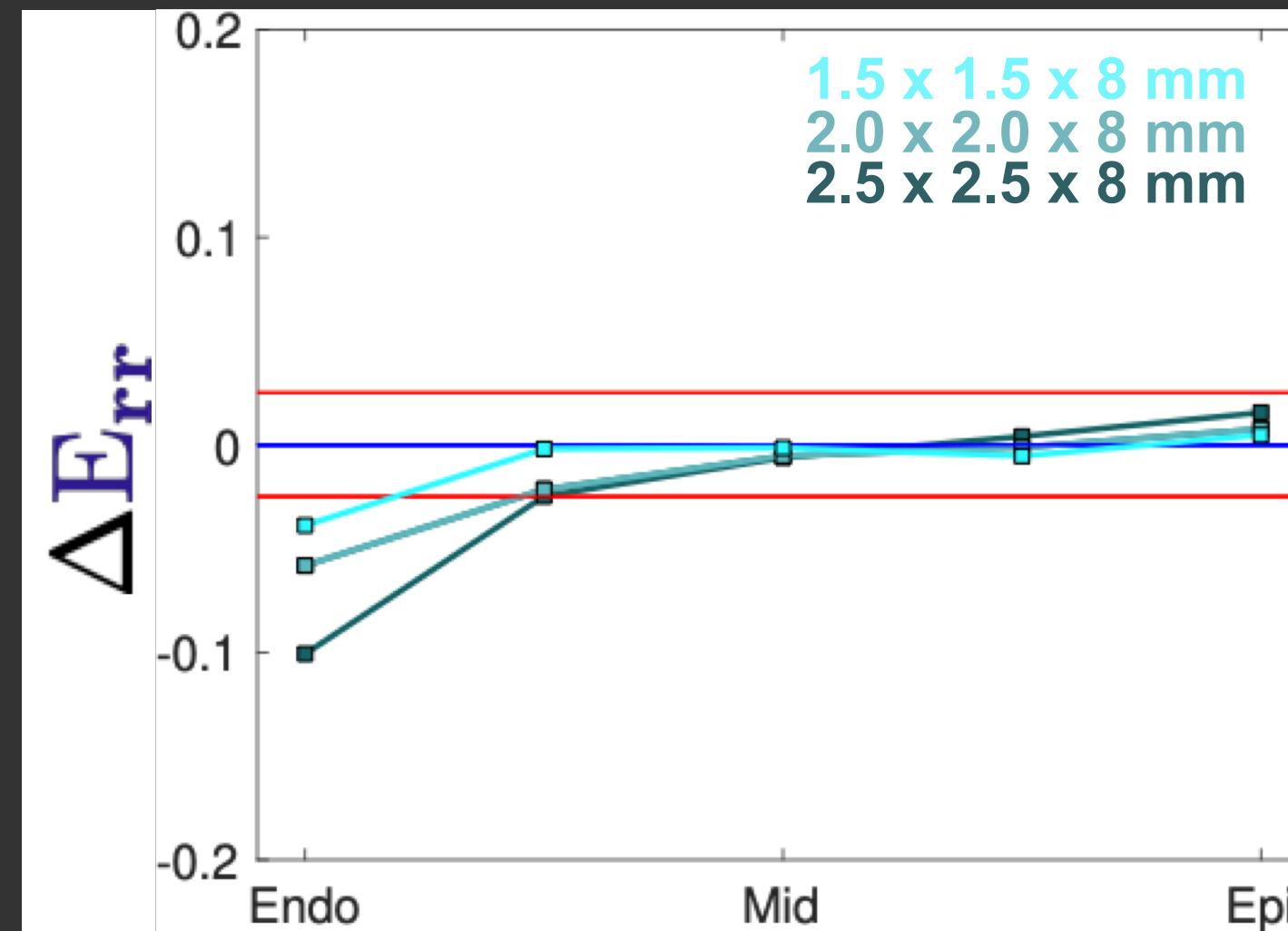
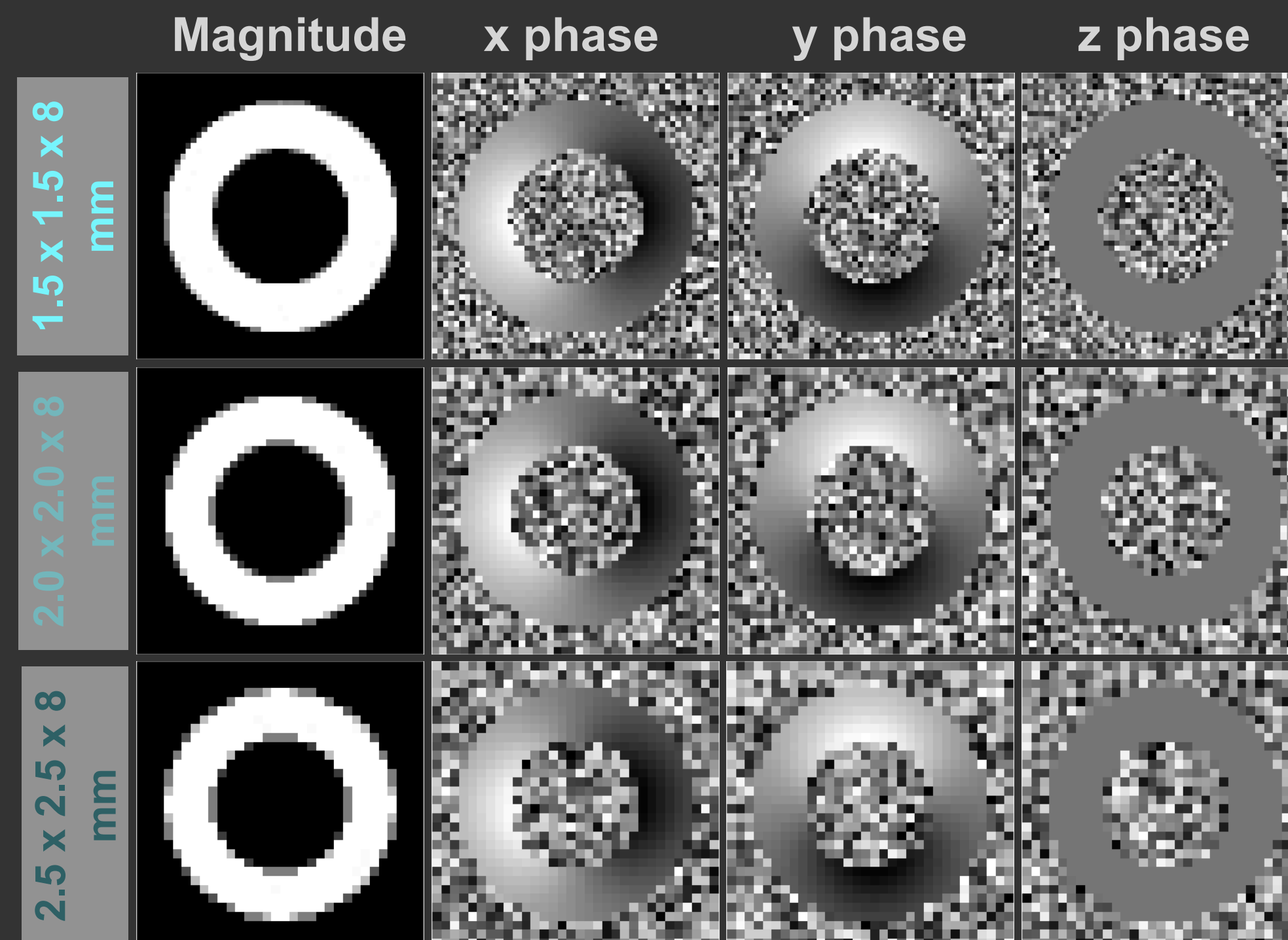


Figure 3- Transmurial ΔE_{rr} across multiple DENSE in-plane resolutions. (top) Median ΔE_{rr} (squares) from epi to endocardium. Blue and red horizontal lines represent, respectively, 0 median strain bias and +0.020 to -0.020 strain tolerance. (bottom) Corresponding peak systolic DENSE magnitude and phase images across multiple in-plane resolutions.



CARDIAC STRAINS FROM DENSE MRI

ACKNOWLEDGEMENTS:

Funding for this work was provided by NIH R01 HL131975 and HL131823 to DBE.

For more information regarding an *in vivo* implementation of this work to compute aggregate cardiomyocyte strain, please see **Program #2104**.



Program #2103



RESULTS

Figure - Cardiomyocyte strain bias vs. wall depth computed at five equidistant transmural points. Squares are strain bias medians and shaded regions are the 95%-CI of strain bias (i.e., the tolerance). Blue and red horizontal lines represent 0 median strain bias and +0.020 to -0.020 strain tolerance, respectively.

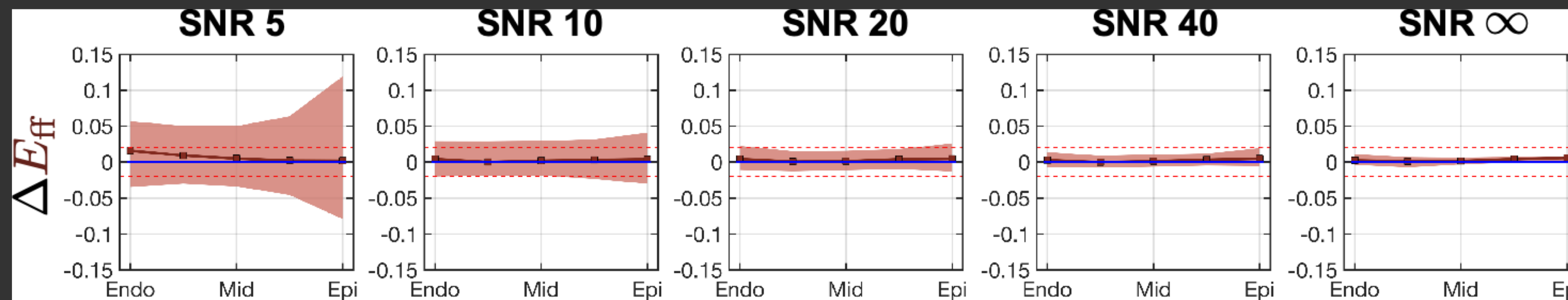
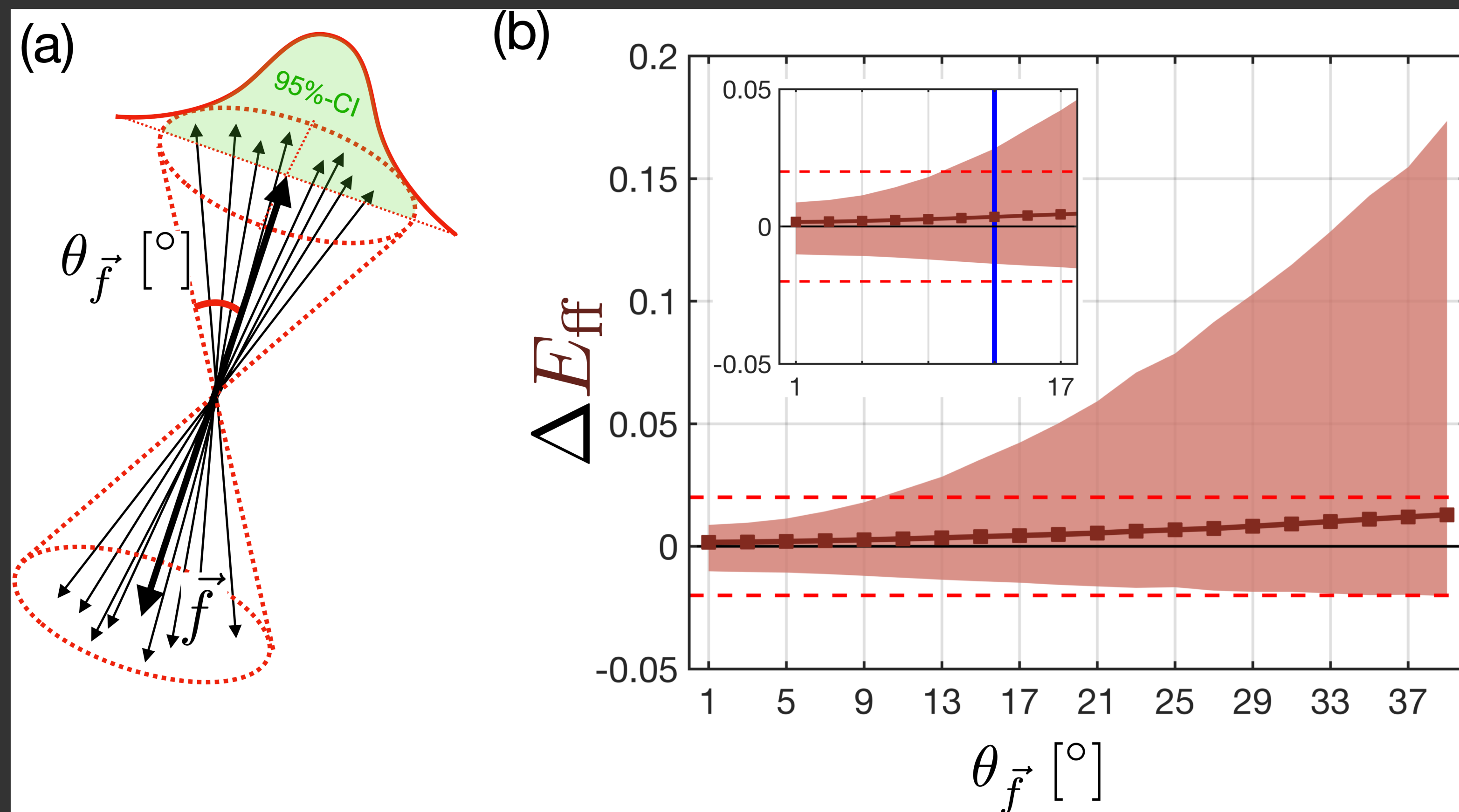


Figure - Results of cardiomyocyte cone of uncertainty analysis. (a) Schematic of cone of uncertainty perturbation. (b) ΔE_{ff} as a function of θ_f . Squares are strain bias medians and shaded regions are the 95%-CI of strain bias (i.e., the tolerance). Red horizontal lines represent +0.020 to -0.020 strain tolerance. Blue vertical line represents θ_f computed from *in vivo* cDTI data



ACKNOWLEDGEMENTS:
Funding for this work was provided by NIH R01 HL131975 and HL131823 to DBE.

For more information regarding an *in vivo* implementation of this work to compute aggregate cardiomyocyte strain, please see **Program #2104.**

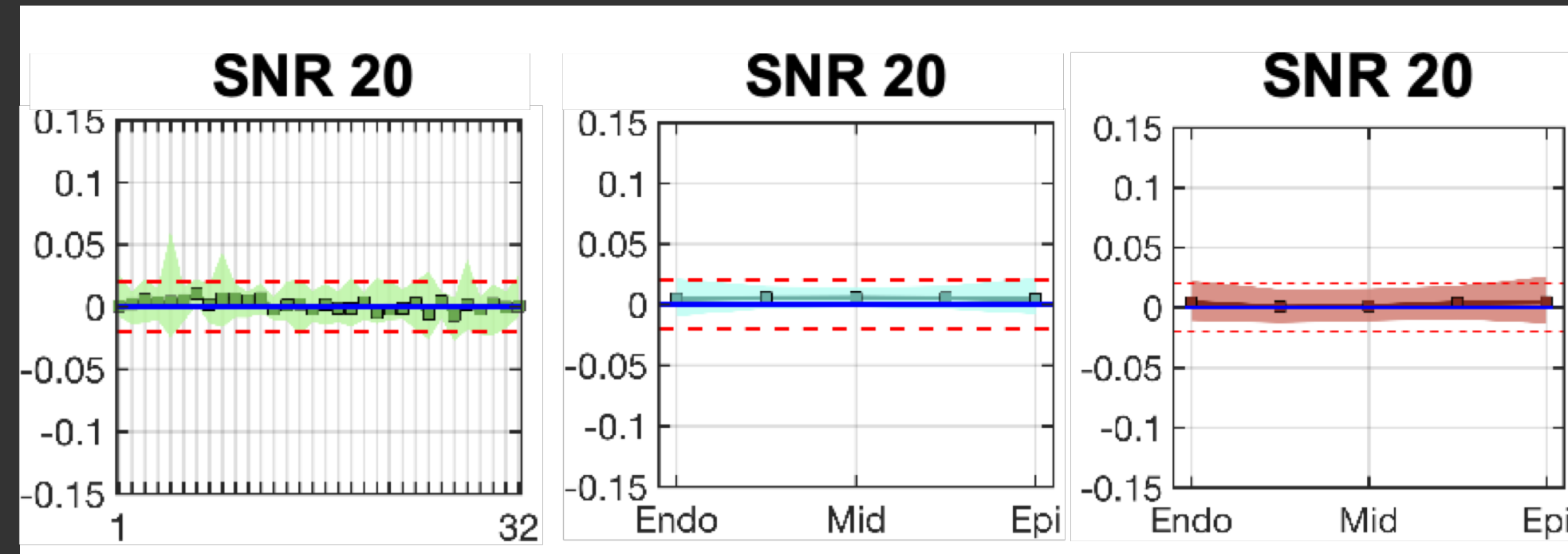


Program #2103

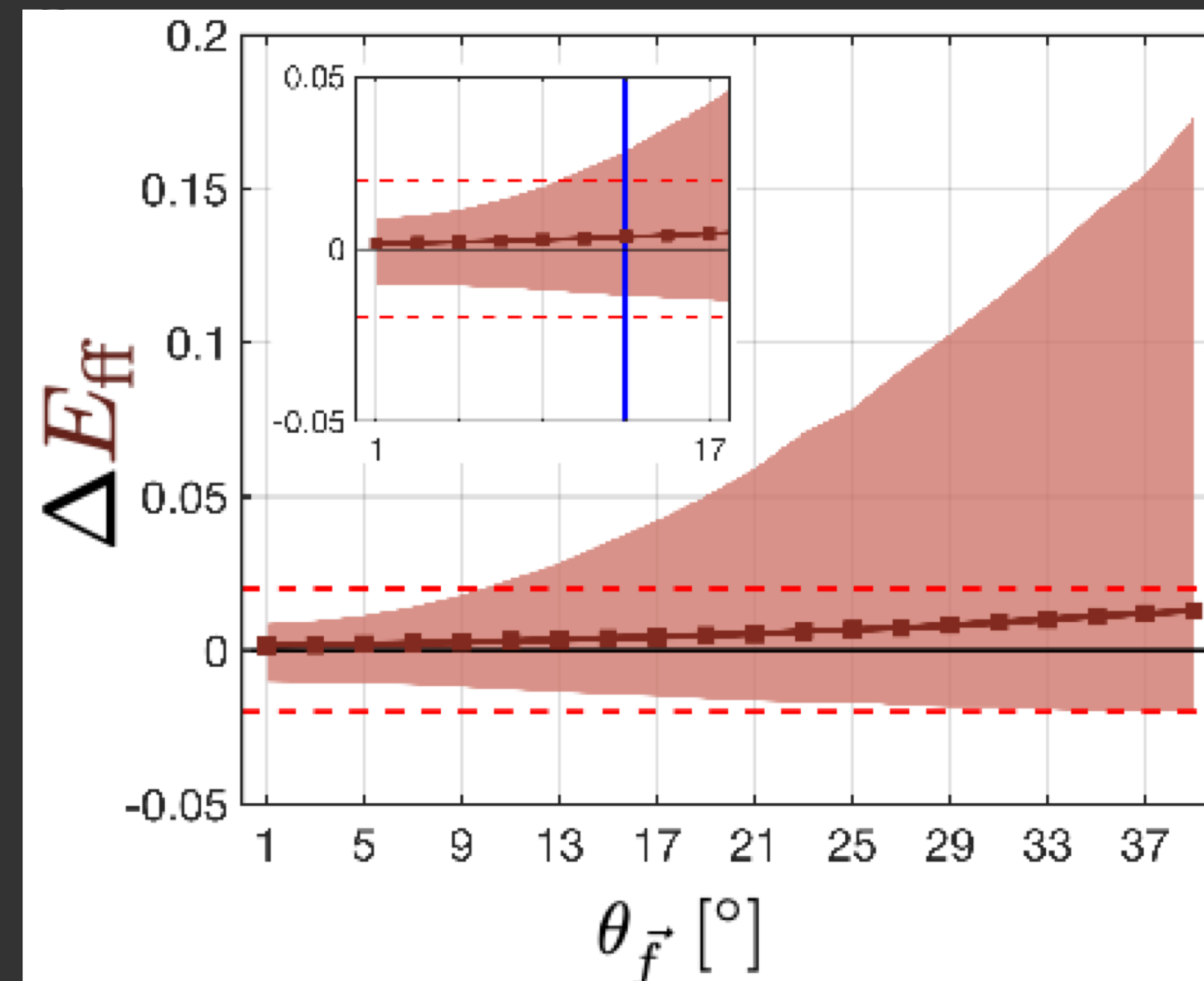
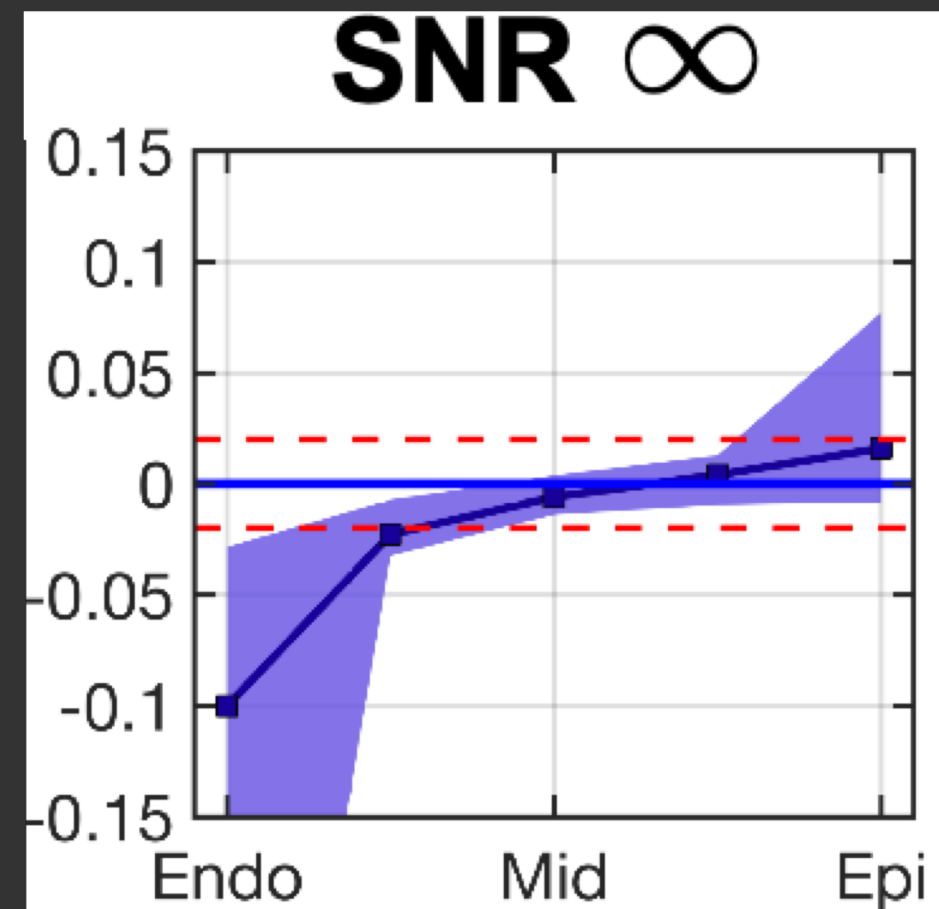


CONCLUSION

E_{ff} , E_{cc} , E_{ll} are computed with near-zero median bias and within a strain tolerance of 0.04 for SNR > 20



E_{rr} exhibited pronounced computed strain bias and a broad 95%-CI even at SNR = Inf



ACKNOWLEDGEMENTS:

Funding for this work was provided by NIH R01 HL131975 and HL131823 to DBE.

For more information regarding an *in vivo* implementation of this work to compute aggregate cardiomyocyte strain, please see **Program #2104**.

E_{ff} is computed with near-zero bias at $\theta_f = 13^\circ$ (computed from *in vivo* cDTI). The upper bound of the 95%-CI of ΔE_{ff} (0.028) is slightly outside the target of +0.02.



Program #2103





Stanford | MEDICINE

Patrick



Dan



Ilya



Nyasha



Mike



Tyler



Matt



Jessica



Kévin



Amanda



iverzh@stanford.edu



Slides